ELSEVIER

European Journal of Pharmacology 448 (2002) 71–80

www.elsevier.com/locate/ejphar

Modeling and biological evaluation of 3,3′-(1,2-ethanediyl)bis[2-(4-methoxyphenyl)-thiazolidin-4-one], a new synthetic cyclooxygenase-2 inhibitor

Rosaria Ottaná [a], Emanuela Mazzon [b], Laura Dugo [c], Francesca Monforte [a], Rosanna Maccari [a], Lidia Sautebin [d], Grazia De Luca [e], Maria Gabriella Vigorita [a], Stefano Alcaro [f], Francesco Ortuso [f], Achille P. Caputi [c], Salvatore Cuzzocrea [c,*]

[a] *Dipartimento Farmaco-chimico, Facoltà di Farmacia, Università di Messina, Vl. SS. Annunziata, Messina 98168, Italy*
[b] *Dipartimento di Biomorfologia, Facoltà di Medicina e Chirurgia, Università di Messina, Policlinico Universitario "G. Martino", Via Consolare Valeria, Messina 98124, Italy*
[c] *Istituto di Farmacologia, Facoltà di Medicina e Chirurgia, Torre Biologica, Università di Messina, Policlinico Universitario "G. Martino", Via Consolare Valeria, Gazzi, Messina 98124, Italy*
[d] *Dipartimento di Farmacologia Universitá "Federico II", Via Domenico Montesano 49, Naples 80131, Italy*
[e] *Istituto di Biochimica e Biochimica Clinica, Facoltà di Medicina e Chirurgia, Università di Messina, Policlinico Universitario "G. Martino", Via Consolare Valeria, Messina 98124, Italy*
[f] *Dipartimento di Scienze Farmacobiologiche, Università "Magna Grœcia" di Catanzaro, Roccelletta di Borgia, Catanzaro, Italy*

Received 1 November 2001; received in revised form 21 May 2002; accepted 24 May 2002

Abstract

Within the series of chiral 3,3′-(1,2-ethanediyl)bis[2-arylthiazolidin-4-ones], the 3,4-dimethoxyphenyl substituted derivative was found in the primary anti-inflammatory screening to be endowed with superior in vivo properties and good safety profile. Such a lead compound was modified by eliminating 3-methoxy group while retaining 4-methoxy group on the aryl rings at 2 and 2′ stereogenic carbons. The 2*R*,2′*S*-meso isomer (VIG3b) of the resulting bisthiazolidinone has been widely investigated. The inhibitory effects on cyclo-oxygenase-1 and cyclo-oxygenase-2 isoenzymes were measured in a human whole blood assay. VIG3b was almost 50 times more selective on the inducible isoform. The cyclo-oxygenase-2 preferential selectivity has been confirmed by modeling VIG3b into the cyclo-oxygenase-1 and cyclo-oxygenase-2 active sites. furthermore, VIG3b was assayed in the experimental model of carrageenan-induced lung injury by evaluating its ability to inhibit: (1) fluid accumulation in the pleural cavity, (2) neutrophil infiltration, (3) prostaglandin E_2 production and (4) lung injury. VIG3b exhibited interesting activity in all these tests.

Keywords: Cyclooxygenase-2; Carrageenan-induced pleurisy; Chemical modeling

1. Introduction

It is known that the inflammatory process is associated with an increase in arachidonic acid metabolites in blood and tissues (Feuerstain and Hallenbeck, 1987). This increase is associated with the de novo synthesis of a new cyclo-oxygenase protein, termed cyclo-oxygenase-2, which is encoded by a gene located on chromosome 1, different from that encoding for the constitutive one (cyclo-oxygenase-1) located on chromosome 9 (Yokohama and Tanabe, 1989; Kosaka et al., 1994). The expression of cyclo-oxygenase-2, induced by inflammatory stimuli in many different cell types, is secondary to the activation of protein tyrosine kinases (Akarasereenont et al., 1995) and of the transcription factor NF-κB (Mitchell et al., 1995).

The current use of nonsteroidal anti-inflammatory drugs (NSAIDs) for the treatment of inflammation and pain is usually accompanied by gastrointestinal ulceration and bleeding, long considered to be inseparably related to the therapeutic effect, since cyclo-oxygenase inhibition was little investigated until the nineties much amount of evidence has now explained that currently available NSAIDs inhibit both cyclo-oxygenase-1 and cyclo-oxygenase-2,

* Corresponding author. Tel.: +39-90-221-3644; fax: +39-90-221-3300.
E-mail address: salvator@www.unime.it (S. Cuzzocrea).

0014-2999/02/$ - see front matter
PII: S0014-2999(02)01888-5

most of them exhibiting selectivity or preference for cyclo-oxygenase-1 (Vane et al., 1994).

The discovery and characterisation of the cyclo-oxygenase-2 isoform (Vane, 1987) suggested that selective inhibition of this enzyme might avoid the side effects of currently available NSAIDs while retaining the therapeutic efficacy. The hypothesis was partially proven when the first selective compounds, NS-398 and DuP-697 were tested in animal models. Both compounds showed anti-inflammatory, analgesic and antipyretic activities, but did not cause gastrointestinal lesions at high doses (Futaki et al., 1993; Copeland et al., 1994). In the last years many different classes of selective cyclo-oxygenase-2 inhibitors have been developed worldwide (Futaki et al., 1993; Gans et al., 1990; Chan et al., 1995). Recently two potent selective cyclo-oxygenase-2 inhibitors, celecoxib and rofecoxib, have demonstrated efficacy in clinical trials of acute pain, osteoarthritis, and rheumatoid arthritis (Simon et al., 1998) and have been marketed in many countries. Both compounds show superior gastrointestinal safety profiles when compared to naproxen, diclofenac or ibuprofen, confirming that the cyclo-oxygenase-2 selectivity mechanism constitutes a promising approach for the treatment of inflammatory diseases.

Based on these considerations, we evaluated this aspect of the biological activity of a novel class of potential NSAIDs with a bisthiazolidinone structure (Previtera et al., 1990). These compounds have in their structure two equivalent stereogenic centres (2 and 2′) bearing aryl or heteroaryl substituents, so they are obtained as 2*R*,2′*R*/2*S*,2′*S* (a) and 2*R*,2′*S*-meso (b) stereomers. They have been assayed as anti-inflammatory agents in the carrageenan-induced rat paw edema, acetic acid-induced whriting and hot plate tests. Mesoforms b generally are more potent than racemates a, both forms showing better safety profiles than indomethacin and phenylbutazone (Previtera et al., 1990; Vigorita et al., 1988).

It was found that (2*R*,2′*S*) 3,3′-(1,2-ethanediyl)bis[2-(3,4-dimethoxyphenyl)-thiazolidin-4-one] had a promising anti-inflammatory activity (“lead” compound) (Vigorita et al., 1997). Aiming to ameliorate this activity, we have differently modified the lead structure. In the lead compound VIG3b (Fig. 1) 3-methoxy groups on the benzene rings were eliminated while 4-methoxy groups were retained. Preliminary screening of VIG3b has shown an improvement of anti-inflammatory activity with good gastrointestinal safety (Vigorita et al., 2001). We then investigated its potential as a selective inhibitor of cyclo-oxygenase-1 and cyclo-oxygenase-2 enzymes in the human whole blood assay, along with the anti-inflammatory effects in the model of rat carrageenan-induced pleurisy. In addition, in order to clarify its interaction modes, VIG3b was modeled into cyclo-oxygenase-1 and cyclo-oxygenase-2 active sites, whose structures have recently been reported (Picot et al., 1994; Kurumbail et al., 1996).

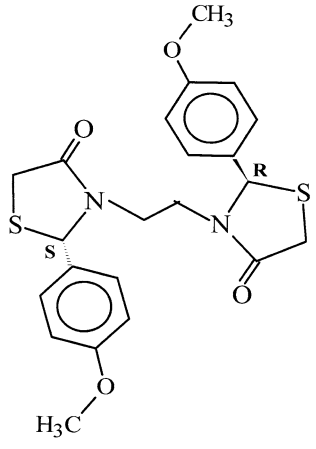

Fig. 1. Structure of 3,3′-(1,2-ethanediyl)bis[2-(4-methoxyphenyl)-thiazolidin-4-one] (VIG3b).

2. Materials and methods

2.1. Synthesis

The preparation of [2*R*,2′*S*-meso]3,3′-(1,2-ethanediyl)-bis[2-(4-methoxyphenyl)-thiazolidin-4-one] followed the general procedure reported by Vigorita et al. (1997). Briefly, to a stirred solution of *N*,*N*′-di-(4-methoxybenzylidene)-ethylenediamine (0.01 mol, 2.96 g) in dry toluene (50 ml), mercaptoacetic acid (0.03 mol, 2.76 g) was added and the mixture was refluxed for 24–48 h. Removal of the solvent in vacuo gave an oily residue which was repeatedly washed with an aqueous solution of Na_2CO_3 (20%) and dried with Na_2SO_4. The crude product (oil) was chromatographed on silica gel columns (diethyl ether: light petroleum 40–60 °C): the first fractions provided the racemate 3a and subsequent ones the mesoform VIG3b. The eluted fractions were dried in vacuo and the solid products were recovered and recrystallised from ethanol.

The 2*R*2′*R*/2*S*2′*S* isomer (3a): yield 56%; m.p. 110–115 °C; IR (nujol, cm^{-1}) 1660 (νC=O); ^{1}H NMR (δ, $CDCl_3$): 2.48, 3.89 (AA′XX′ system, CH_2–CH_2), 3.66, 3.71 (AB system, *J*=15.5, 5,5′CH_2), 3.79 (s, 3H OCH_3), 5.91 (s, 2H, 2,2′CH), 6.84, 7.29 (m, 4H, aromatic protons).

The 2*R*2′*S*-meso isomer (VIG3b): yield 38%; m.p. 180–185 °C; IR (nujol, cm^{-1}) 1668 (νC=O); ^{1}H NMR (δ, $CDCl_3$): 2.79, 3.61 (AA′XX′ system, CH_2–CH_2), 3.65, 3.74 (AB system, *J*=15.5, 5,5′CH_2), 3.82 (s, 3H OCH_3), 5.55 (s, 2H, 2,2′CH), 6.90, 7.25 (m, 4H, aromatic protons).

2.2. Computation

To explore the interaction between VIG3b and the cyclo-oxygenase-1 and cyclo-oxygenase-2 enzymes, the crystallographic models of such macromolecules deposited in the Protein Data Bank (PDB) were studied. The models 1CQE (1CQE is the complex between ovine cyclo-oxygenase-1 and flurbiprofen obtained at a resolution of 3.10) (Picot et

al., 1994) and 6COX (6COX is the complex between murine cyclo-oxygenase-2 and SC-558 obtained at a resolution of 3.0 Å) (Kurumbail et al., 1996), related respectively to cyclo-oxygenase-1 and cyclo-oxygenase-2 co-crystals with non-covalent ligands were selected, as then had the lowest resolution factor with respect to other available PDB structures. Crystallographic models of both cyclo-oxygenase isozymes obtained with the same level of resolution factor have recently been used for a computational study (Palomer et al., 2000).

Detailed analysis of the ligand binding modes into the selected Protein Data Bank models allowed us to identify the aminoacid residues responsible for recognition of the inhibitor. We considered the aminoacids within 10 Å from the crystallographic position of each ligand in the original PDB structures. Both cyclo-oxygenase-1 and cyclo-oxygenase-2 catalytic sites are delimited by the Tyr^{385} residue that hinders the heme group from the ligand position. Therefore, we excluded it from our models. Following this procedure two reduced models were obtained, taking into account 73 and 87 aminoacid residues for cyclo-oxygenase-1 and cyclo-oxygenase-2, respectively.

The starting geometries of the enzyme–inhibitor [E·I] complexes were generated by placing an energy minimized conformation of the ligand into the binding site. These complexes were submitted to 100 ps of molecular stochastic dynamic mix-mode simulations (Guarnieri and Still, 1994) at 300° K using an Amber* force field (McDonald and Still, 1992) as implemented in the MacroModel package (MacroModel version 5.5 for SGI) (Mohamadi et al., 1990). In these calculations, we constrained the enzyme atoms applying the standard force constant of 100 kJ/mol. No constraint was applied to the inhibitor. We preferred to keep the protein 3D structure of both enzymes rigid, because we wanted to keep our model as close as possible to the original X-ray structures. Using this approach, we have found good correlations between drug-enzyme interaction energies and the experimental biological data.

In order to relax the internal degrees of freedom of the ligand, the conformations generated by the previous steps were minimized with the same force field and constraint.

Finally, the enzyme–ligand interaction energies were calculated with the MOLINE package (Alcaro et al., 2000) using the same molecular mechanics parameters of the Amber* force field. The internal energies of the ligand were extrapolated from the conformations assumed by the inhibitor in the global minima obtained after the mix-mode and enzyme-constrained simulations.

2.3. Animals

Male Sprague–Dawley rats (300–350 g; Charles River; Milan; Italy) were housed in a controlled environment and provided with standard rodent chow and water.

Animal care was in compliance with Italian regulations on protection of animals used for experimental and other scientific purposes (D.M. 116192) as well as with the EEC regulations (O.J. of E.C. L 358/1 12/18/1986).

2.4. Cyclo-oxygenase-1 activity in human whole blood

Whole blood was drawn from donors when they had not taken any NSAIDs during the 2 weeks preceding the study. One-milliliter aliquots of whole blood were immediately transferred into glass tubes and allowed to clot at 37 °C for 60 min. Serum was separated by centrifugation (10 min at 2000 rpm) and kept at −80 °C until assayed for thromboxaneB_2. Whole blood thromboxaneB_2 production was measured by enzyme immunoassay (EIA) as a reflection of the cyclooxygenase activity of the platelet cyclo-oxygenase-1 maximally stimulated by endogenously formed thrombin (Patrono et al., 1980).

2.5. Cyclo-oxygenase-2 induction in human whole blood

One-milliliter aliquots of whole blood samples from the same donors, containing 10 IU of sodium heparin were incubated in both the absence and presence of lipopolysaccharide (10 μg/ml) for 24 h at 37 °C. The contribution of platelet cyclo-oxygenase-1 was suppressed by adding acetyl salicylic acid (10 μg/ml) at time 0. Plasma was separated by centrifugation (10 min at 2000 rpm) and kept at −80 °C until assayed for prostaglandin E_2. Prostaglandin E_2 production by lipopolysaccharide-stimulated monocytes was measured by EIA.

2.6. Effects of cycloxygenase inhibitor VIG3b

The compound to be tested was dissolved in ethanol and 0.30-μl aliquot of the solution was pipetted directly into test tubes to a final concentration of $10^{-8}/10^{-5}$ M. The solvent was evaporated and 1-ml aliquots of heparinized whole blood were added. The effects of VIG3b on cyclo-oxygenase-2 activity were studied by incubating the compound at four different concentrations with multiple heparinized whole blood samples in the presence of lipopolysaccharide (10 μg/ml) for 24 h, whereas the effects on cyclo-oxygenase-1 activity were evaluated by incubating VIG3b the compound at four different concentrations with multiple whole blood samples that were allowed to clot at 37 °C for 60 min.

The results were expressed as percentage inhibition versus control (inhibitor absence) and the cyclo-oxygenase-1/cyclo-oxygenase-2 selectivity is given as IC_{50} cyclo-oxygenase-1/IC_{50}cyclo-oxygenase-2 ratio.

2.7. Carrageenan-induced pleurisy

The rats were anaesthetised with isoflurane and a skin incision was mode at the level of the left sixth intercostal space. The underlying muscle was dissected and saline (0.2 ml) or saline containing 1% λ-carrageenan (0.2 ml) was

injected into the pleural cavity. The skin incision was closed with a suture and the animals were allowed to recover. VIG3b (5–20 mg/kg), or an equivalent volume (0.3 ml) of vehicle (dimethyl sulfonic acid, DMSO), was administered intraperitoneally (i.p.) 5 min before carrageenan. At 4 h after the injection of carrageenan, the animals were killed by inhalation of CO_2. The chest was carefully opened and the pleural cavity was rinsed with 2 ml of saline solution containing heparin (5 U/ml) and indomethacin (10 μg/ml). The exudate and washing solution were removed by aspiration and the total volume was measured. Any exudate contaminated with blood was discarded. The amount of exudate was calculated by subtracting the volume injected (2 ml) from the total volume recovered. The leukocytes in the exudate were suspended in phosphate-buffer saline (PBS) and counted with an optical microscope in a Burker's chamber after vital Trypan Blue staining.

2.8. Measurement of lung-tissue myeloperoxidase activity and malondialdehyde levels

The activity of myeloperoxidase, a hemoprotein located in azurophil granules of neutrophils, was used as a biochemical marker for neutrophil infiltration into tissues (Bradley et al., 1982).

Myeloperoxidase activity was measured photometrically by a method similar to that described previously (Laight et al., 1994). At 4 h following the intrapleural injection of carrageenan, lung tissues were obtained and weighed. Each piece of tissue was homogenized in a solution containing 0.5% hexa-decyl-trimethyl-ammonium bromide dissolved in 10 mM potassium phosphate buffer (pH 7.00) and centrifuged for 30 min at 20,000×*g* at 4 °C. An aliquot of the supernatant was then allowed to react with a solution of tetramethylbenzidine (1.6 mM) and 0.1 mM H_2O_2. The rate of change in absorbance was measured spectrophotometrically at 650 nm. Myeloperoxidase activity was defined as the quantity of enzyme degrading 1 μmol of peroxide/min at 37 °C and was expressed in milliunits per 100 mg weight of wet tissue. Malondialdehyde levels in the lung tissue were determined as an indicator of lipid peroxidation (Ohkawa et al., 1979).

Lung tissue, collected at the time specified, was homogenized in 1.15% KCl solution. An aliquot (100 μl) of the homogenate was added to a reaction mixture containing 200 μl of 8.1% SDS, 1500 μl of 20% acetic acid (pH 3.5), 1500 μl of 0.8% thiobarbituric acid and 700 μl distilled water. Samples were then boiled for 1 h at 95 °C and centrifuged at 3000×*g* for 10 min. Absorbance of the supernatant was measured by spectrophotometry at 650 nm.

2.9. Histological examination

Lung biopsies were taken at 4 h after injection of carrageenan. The biopsies were fixed for 1 week in buffered formaldehyde solution (10% in phosphate buffered saline) at room temperature, dehydrated in an ethanol gradient and embedded in Paraplast (Sherwood Medical, Mahwah, NJ). Tissue sections (thickness 7 μm) were deparaffinized with xylene, stained with trichromic Van Gieson and studied using light microscopy (Dialux 22 Leitz).

2.10. Measurement of cytokines

Tumor necrosis factor-α (TNF-α) and interleukin-1β levels were evaluated in the exudate at 4 h after the induction of pleurisy by carrageenan injection. The assay was carried out with a colorimetric, commercial kit (Calbiochem-Novabiochem, USA). The ELISA has a lower detection limit of 10 pg/ml.

2.11. Assessment of cyclo-oxygenase activity

Lungs were obtained at 24 h after the induction of pleurisy by carrageenan injection. The tissue was homogenised at 4 °C in a buffer containing the following protease inhibitors are: Hepes Buffer 20 mM pH 7.2 + Sucrose 320 mM, DTT 1 mM, STY 10 ug/ml, aprotinin 2 ug/ml, leupeptin 10 ug/ml in a ratio of 5:1 (v/w). The protein concentration in the homogenates was measured by the Bradford assay (Bradford, 1976), with bovine serum albumin as standard. Homogenates were incubated at 37 °C for 30 min in the presence of excess arachidonic acid (30 μM). The samples were boiled and centrifuged at 10,000×*g* for min. The concentration of 6-keto-prostaglandin $F_{1\alpha}$ present in the supernatant was measured by radioimmunoassay as previously described (Tomlinson et al., 1994).

2.12. Measurement of prostaglandin e_2 in the pleural exudate

The amount of prostaglandin E_2 present in the pleural fluid was measured by radioimmunoassay without prior extraction or purification (Sautebin et al., 1995).

2.13. Materials

Cell culture medium, heparin and fetal calf serum were obtained from Sigma (Milan, Italy). Perchloric acid was obtained from Aldrich (Milan, Italy). All other reagents and compounds used were obtained from Sigma.

2.14. Data analysis

All values in the figures and text are expressed as means ± standard error of the mean (S.E.M.) for *n* observations. For the in vitro studies, the data represent the number of wells studied (six to nine wells from two to three independent experiments). For the in vivo studies, *n* represents the number of animals studied. The results were analysed by one-way analysis of variance (ANOVA) followed by a Bonferroni's post-hoc test for multiple compar-

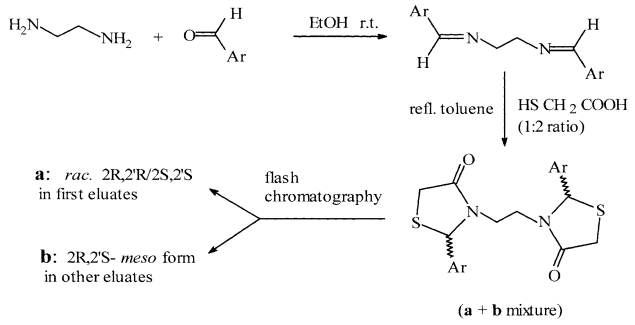

Fig. 2. Synthesis.

isons. A P value less of than 0.05 was considered significant. In the experiments involving histology, the figures shown are representative of at least three experiments performed on different experimental days.

3. Results

3.1. Chemistry

To prepare (2*R*,2′*S*)3,3′-(1,2-ethanediyl)bis[2-(4-methoxyphenyl)-thiazolidin-4-one] VIG3b, synthetic procedures previously reported were followed (Fig. 2). The 2*R*,2′*S*-meso isomer (VIG3b) was obtained in small yields and had a higher melting point than the enantiomeric pair 2*R*,2′*S*/2*S*,2′*S*. As is usual in bisthiazolidinone series, the stereochemistry of both diastereomers was assigned on the basis of the ^{1}H NMR spectra characteristics: in particular, the isochronism of the corresponding protons in the heterocyclic rings, the 2,2′-CH resonance of the *R*,*R*/*S*,*S* racemate at higher frequencies than those of the meso-isomer ($\Delta_V \cong 0.35$ ppm in $CDCl_3$) and the difference in the resonance of the heterotopic geminal protons of the ethylene chain that resonate as AA′XX′ systems (Vigorita et al., 1997). These assignments, in turn, were supported by X-ray crystallographic analysis of analogues (Benetollo et al., 1991, 1998).

3.2. Computation study

The conformational search described in the experimental section was applied to model the interactions of VIG3b with cyclo-oxygenase-1 and cyclo-oxygenase-2 active sites. On the basis of the structures of co-crystallized complexes (Picot et al., 1994; Kurumbail et al., 1996), the energetic data expressed as enzyme-inhibitor interaction and ligand internal energies are displayed in Table 1, together with two significant geometrical descriptors of VIG3b conformations modeled into the binding sites of the enzymes. VIG3b can interact with both enzymes but it shows a significant preference for the cyclo-oxygenase-2 isoform; in fact, binding into the cyclo-oxygenase-2 cleft is more stabilized than in the cyclo-oxygenase-1 cavity with ΔE of about 10 kcal/mol. The ligand internal energy of VIG3b into the cyclo-oxygenase-2 binding site is also entropically favored, as shown in Table 1, where the ΔE (internal) is more than 5 kcal/mol.

In order to understand the reasons for such a trend, we analyzed in detail the structural differences in binding sites between the cyclo-oxygenase-1 and cyclo-oxygenase-2 enzymes. According to Kurumbail et al. (1996), the most important influence is due to the amino acid residue 523. Such a non-conserved residue in cyclo-oxygenase-1 is an Ile and in cyclo-oxygenase-2, a Val. Due to this replacement, a supplementary small cleft is available in cyclo-oxygenase-2 to accommodate the ligands.

Fig. 3 shows the role of the residue Ile^{523} which blocks access into the cyclo-oxygenase-1 minor cavity of the binding site with respect to the Val^{523} in cyclo-oxygenase-2. The conformation induced effect of VIG3b is remarkable: in cyclo-oxygenase-1 it assumes a folded conformation and in cyclo-oxygenase-2, an extended one (see Table 1). The most representative residues involved in the recognition of VIG3b with both sites are shown in Fig. 3.

In conclusion, the differently accessible volumen of the crucial area in the clefts, as shown in Fig. 3, are responsible for the ligand energy stabilization and its conformation into the binding site. Both interaction and internal energies are affected by this sterically driven diversity as described in Table 1 and clearly indicate the preference of VIG3b for interaction with the cyclo-oxygenase-2 isoform.

3.3. Evaluation of VIG3b on cyclo-oxygenase-1 and cyclo-oxygenase-2 activity

VIG3b showed marked selectivity for cyclo-oxygenase-2 in the human whole blood assay (Bradley et al., 1982). Its IC_{50} on cyclo-oxygenase-2 was 1.12 μM while on cyclo-oxygenase-1 it was 53.7 μM. The ratio of cyclo-oxygenase-1/cyclo-oxygenase-2 selectivity was thus 47.9.

3.4. Effects of VIG3b in carrageenan-induced pleurisy

Compared to lung sections from saline-treated animals, those from rats treated with carrageenan revealed significant tissue damage on histological examination. They showed edema, tissue injury as well as infiltration of the tissue with neutrophils (Fig. 4A). The new compound (VIG3b) at the

Table 1
Geometrical descriptors[a], E/L interaction and ligand internal energies of VIG3b

	Ar/Ar distance (Å)	N–C–C–N dihedral angle(°C)	Enzyme/ligand interaction energy (kcal/mol)	Ligand internal energy (kcal/mol)
COX-1	4.94	40.2	−33.2	6.22
COX-2	7.47	−150.8	−43.82	0.68

[a] In global minimum conformations within the enzyme clefts.

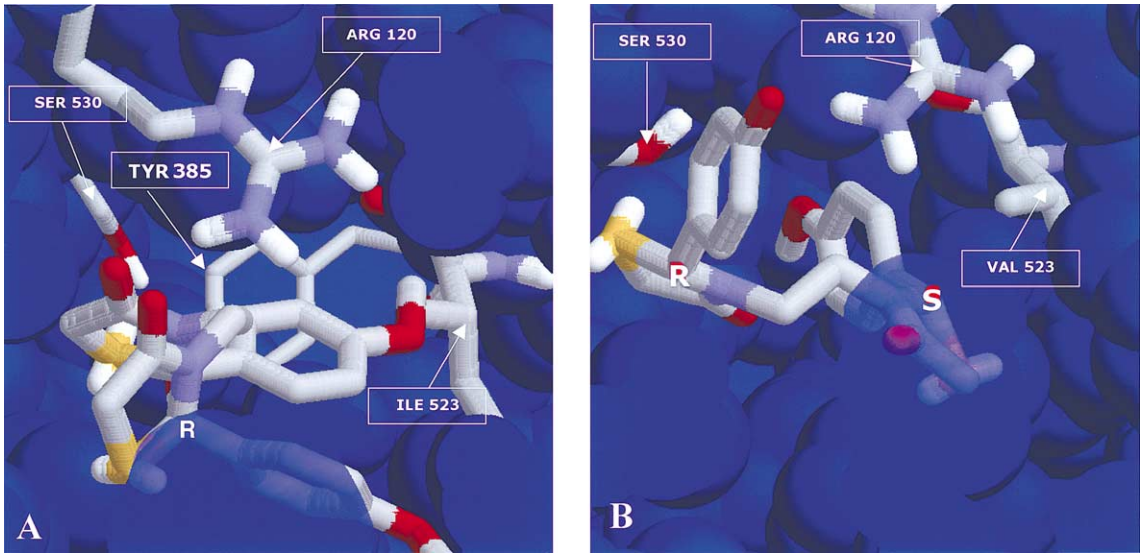

Fig. 3. Minimum energy conformations of VIG3b into the cyclo-oxygenase-1 (A) and cyclo-oxygenase-2 (B) binding clefts. The ligand and the most important amino acid residues of the enzymes are labeled and displayed by polytube representation; other sterically important residues in the binding clefts are shown in blue as CPK models.

highest dose tested (20 mg/kg, intraperitoneally, i.p.), significantly reduced the degree of injury as well as neutrophil infiltration (Fig. 4B). Furthermore, the injection of carrageenan into the pleural cavity of rats elicited an acute inflammatory response characterized by the accumulation of fluid (edema) containing a large amounts of neutrophils (Fig. 5A and B). Neutrophils also infiltrated the lung tissues (Fig. 6A) and this was associated with lipid peroxidation of lung tissues as evidenced by the increased levels of malonyldialdehyde (Fig. 6B). Edema, neutrophil infiltration in lung tissue and lipid peroxidation were attenuated in a dose-dependent fashion by the oral administration of VIG3b (5–20 mg/kg, n=10) (Figs. 4–6).

3.5. Effects of VIG3b on the release of cytokines

When compared to controls at 4 h after the injection of carrageenan, an increase in the levels of TNF-α and interleukin-1β was observed in pleural exudates (Fig. 7A and B). Cytokine production was attenuated in a dose-dependent fashion by the administration of VIG3b (5–20 mg/kg, n=10).

3.6. Effects of VIG3b on the release of prostaglandins

The cyclo-oxygenase-2 activity in carrageenan-induced pleural exudate and lung homogenates was assessed by

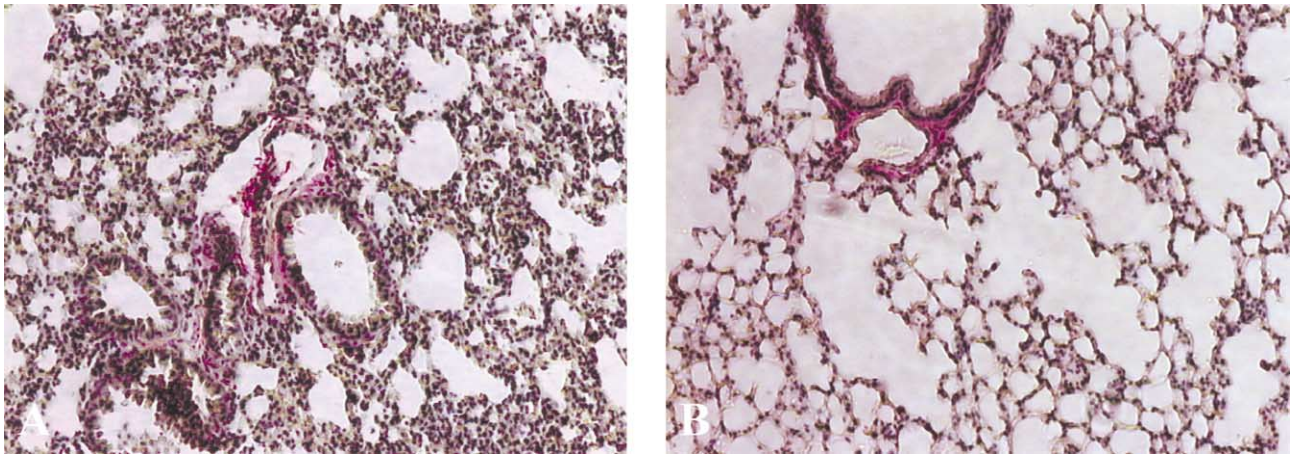

Fig. 4. Effect of VIG3b on lung injury: When compared to lung sections taken from carrageenan-treated rats (A) demonstrates interstitial hemorrhage and polymorphonuclear leukocyte accumulation. Lung sections from a carrageenan-treated rat that had received VIG3b (20 mg/kg) (B) exhibit reduced interstitial hemorrhage and less cellular infiltration. Original magnification: ×125. Figure is representative of at least three experiments performed on different experimental days.

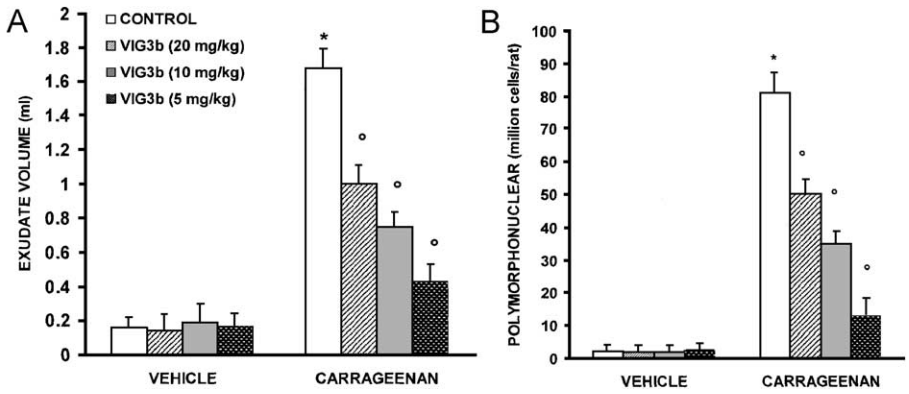

Fig. 5. Effect of VIG3b on carrageenan-induced inflammation: The increase in volume exudate (A) and accumulation of polymorphonuclear cells (B) in the pleural cavity at 4 h after carrageenan injection was inhibited in a dose-dependent manner by VIG3b (5–20 mg/kg). Each value is the mean±S.E.M. for n=10 experiments. *P<0.01 vs. sham. °P<0.01 vs. carrageenan.

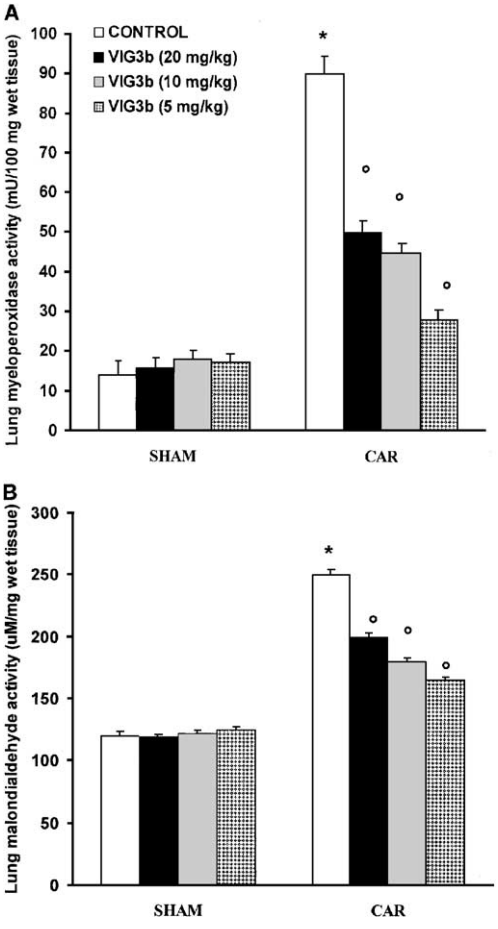

Fig. 6. Effect of VIG3b on myeloperoxidase activity and malondialdehyde levels in the lung. Within 24 h, pleural injection of carrageenan led to an increase in neutrophil accumulation in the lung (as measured by myeloperoxidase activity, A) an effect that was associated with increased lipid peroxidation of lung tissue (as measured by malondialdheyde, B). VIG3b inhibited in a dose-dependent (5–20 mg/kg) fashion neutrophil infiltration and lipid peroxidation. Each value is the mean±S.E.M. for n=10 experiments. *P<0.01 vs. sham. °P<0.01 vs. carrageenan.

measuring the increase in the formation of prostaglandin E_2 in the exudate. The amounts of prostaglandin E_2 found in the pleural exudate of carrageenan-treated rats was 255±12 pg/rat (n=10). Prostaglandin E_2 levels were significantly

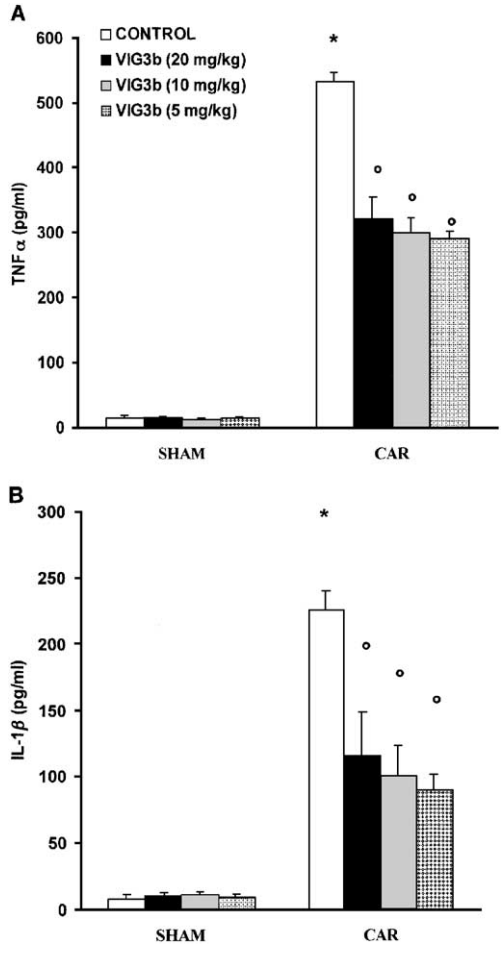

Fig. 7. Pleural injection of carrageenan caused after an increase in the release of the cytokines, tumor necrosis factor alpha (TNF-α, A) and interleukin-1β (B). VIG3b (5–20 mg/kg) significantly inhibited TNF-α and interleukin-1β. Each value is the mean±S.E.M. for n=10 experiments. *P<0.01 vs. sham. °P<0.01 vs. carrageenan.

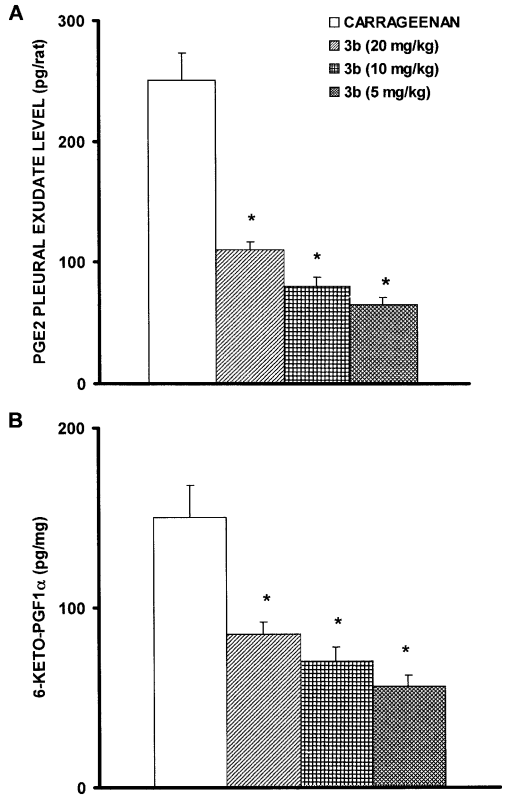

Fig. 8. Prostaglandin E_2 levels in the pleural exudate (A) and 6-keto-prostaglandin $F_{1\alpha}$ in the lungs (B) from carrageenan-treated rats. The amounts of prostaglandin E_2 and 6-keto-prostaglandin $F_{1\alpha}$ were significantly reduced in a dose dependent manner in rats treated with VIG3b (5–20 mg/kg). Data are means±S.E.M. means for 10 rats for each group. *P<0.01 vs. sham. °P<0.01 vs. carrageenan.

lower in the exudate obtained from carrageenan-treated rats which had been treated with VIG3b. In lungs from carrageenan-treated rats, the amount of 6-keto-prostaglandin $F_{1\alpha}$ was 179±9 pg/mg/tissue (Fig. 8A), but it was significantly reduced in lungs from carrageenan-treated rats which had been treated with VIG3b (Fig. 8B).

4. Discussion

In the present study, we demonstrated that the new bisthiazolidinone compound, VIG3b, is a better cyclo-oxygenase-2 inhibitor than the lead compound of this class (Fig. 1), as the results from human whole blood assay and com putational study indicate. In particular, the cyclo-oxygenase-1/cyclo-oxygenase-2 selectivity ratio of VIG3b (47.8) is more than 30 times higher than the same ratio for the lead compound, 1.51. Thus VIG3b can be classed among the partially selective cyclo-oxygenase-2 inhibitors on the basis of its cyclo-oxygenase-1/cyclo-oxygenase-2 selectivity ratio (Warner et al., 1999).

In addition, theoretical evidence was obtained when the flexible structure of VIG3b was modeled into binding sites of both enzymes, on the basis of the structures reported by Picot et al. (1994) and Kurumbail et al. (1996). In the cyclo-oxygenase-2 hydrophobic channel, VIG3b assumes the extended conformation, having a N–C–C–N dihedral angle of −150.8° and an internal energy of only 0.68 kcal/mol. (Table 1). The corresponding data for the lead compound are very different: N–C–C–N dihedral angle=59.4° and ligand internal energy=28.93 kcal/mol (Ottanà et al., 2001). Together, these results account well for the better cyclo-oxygenase-2 selectivity of VIG3b.

From the pharmacological point of view, the results from the carrageenin-induced pleurisy assay indicate that the development of lung inflammation in induced pleurisy is associated with prostaglandin production in affected tissues. It is known that the regulation of cyclo-oxygenase-2 gene expression involves both transcriptional and translational mechanisms (Raz et al., 1989), but details of the mechanisms remain elusive. (Ristimaki et al., 1994) Recently it was shown that interleukin-lβ induces a rapid but transient activation of cyclo-oxygenase-2 transcription in inflammatory cells and stabilizes the cyclo-oxygenase-2 mRNA in the absence of transcription. It is likely that carrageenan induces the production of interleukin-1β as well as TNF-α in the exudate (Cuzzocrea et al., 1999) and that interleukin-1β and TNF-α play an important role in the regulation of sustained cyclo-oxygenase-2 polypeptide synthesis in inflammatory responses.

Therefore, the in vivo administration of VIG3b to carrageenan-treated animals rapidly reversed exudate formation, reduced lung inflammation and returned prostaglandin E_2 levels to normal. Furthermore, VIG3b diminished the level of cyclo-oxygenase-2 activity in lung tissue, suggesting that prostaglandins enhance the local expression of cyclo-oxygenase-2 itself in inflamed lung tissue. The development of lung injury was also associated with increased levels of TNF-α and interleukin-1β in the exudate. Treatment of carrageenan-treated rats with VIG3b markedly reduced the level of TNF-α and interleukin-1β in the exudate. Partial inhibition of systemic cytokines production by treatment with indomethacin has been documented (Theisen-Popp et al., 1992). Both enhancement and suppression of TNF-α production have been demonstrated to be dose-dependently regulated by prostaglandinE_2 and cAMP in rat peritoneal macrophages (Renz et al., 1988). In addition, treatment with VIG3b markedly reduced (1) the cellular infiltrate in the pleural cavity as well as in the lung, and (2) inflammation of lung tissue. The ability of cyclo-oxygenase inhibitors to partially reduce the inflammatory cell infiltrate in the lung could partly explain the observed reduction in the levels of cyclo-oxygenase-2 and cytokine production.

Moreover, lung inflammation is usually characterised by an extensive infiltration of pulmonary tissue by polymorphonuclear leukocytes, which is more marked in bronchoalveolar lavage fluid during acute, infectious exacerbations. Neutrophil activation represents an important source of reactive oxygen species (Cuzzocrea et al., 2001).

Furthermore, there is much evidence that the production of reactive oxygen species such as hydrogen peroxide, superoxide and hydroxyl radicals at the site of inflammation contributes to tissue damage (Cuzzocrea et al., 2001). Using the experimental model described here, previous work has demonstrated the anti-inflammatory potential of various therapeutic approaches aimed at the inhibition of NO synthesis, peroxynitrite and reactive oxygen species formation (Cuzzocrea et al., 2001).

In the present study, we have found that VIG3b reduced lipid peroxidation; this effect is more likely to be related to the reduced mononuclear cell infiltration.

As with most pharmacological cyclo-oxygenase inhibitors, however, we cannot exclude additional, prostaglandin-independent effects which may have contributed to the anti-inflammatory effects observed with VIG3b in the current study.

At the present time, our findings support a model in which carrageenan induces local TNF-α, cyclo-oxygenase-2 and interleukin-1β production during experimental pleurisy, and these results support the view that the overproduction of cyclo-oxygenase-2-derived prostaglandins contributes to acute inflammation.

Taken together our results point to VIG3b as a representative compound of a new class of cyclo-oxygenase-2 inhibitors with bisthiazolidinone structure. VIG3b as such, or as further optimised derivatives, could be useful in the therapy of conditions associated with local or systemic inflammation.

References

Akarasereenont, P., Bakhle, Y.S., Thiemermann, C., Vane, J.R., 1995. Cytokine-mediated induction of cyclo-oxygenase-2 by activation of tyrosine kinase in bovine endothelial cells stimulated by bacterial lipopolysaccharide. Br. J. Pharmacol. 115, 401–408.

Alcaro, S., Gasparrini, F., Incani, O., Mecucci, S., Misiti, D., Pierini, M., Villani, C.A., 2000. A quasi-flexible automatic docking processing for studying stereoselective recognition mechanisms: Part I. Protocol validation. J. Comp. Chem. 21, 515–530.

Benetollo, F., Bombieri, G., Del Prà, A., Basile, M., Previtera, T., Vigorita, M.G., 1991. Structures of the configurational isomers of 3,3′(1,2-ethanediyl)bis[2(3-fluorophenyl)-1,3-thiazolidine-4-one]. J. Crystallogr. Spectrosc. Res. 21, 113–120.

Benetollo, F., Bombieri, G., Del Pra, A., Orsini, F., Previtera, T., Vigorita, M.G., 1998. Structural and conformational studies on 3,3′-bis[1,3-thiazolidine-4-one] derivatives with biological activity. J. Mol. Struct. 443, 131–139.

Bradford, M.M., 1976. A rapid and sensitive method for the quantitation of microgram quantities of protein utilizing the principle of protein-dye binding. Anal. Biochem. 72, 248–252.

Bradley, P.P., Priebat, D.A., Christensen, R.D., Rothstein, G., 1982. Measurement of cutaneous inflammation: estimation of neutrophil content with an enzyme marker. J. Invest. Dermatol. 78, 206–209.

Chan, C., Boyce, S., Brideau, C., Ford-Hutchinson, A.W., Gordon, R., Guay, D., Hill, R.G., Li, C., Mancini, J., Penneton, M., Prasit, P., Rasori, R., Rieneau, D., Roy, P., Tagari, P., Vickers, P., Wong, E., Rodger, I.W., 1995. Pharmacology of a selective cyclooxygenase-2 inhibitor, L-745,337: a novel nonsteroidal anti-inflammatory agent with an ulcerogenic sparing effect in rat and nonhuman primate stomach. J. Pharmacol. Exp. Ther. 274, 1531–1537.

Copeland, R.A., Williams, J.M., Giannaras, J., Nurnberg, S., Covington, M., Pinto, D., Pick, S., Trazkos, J.M., 1994. Mechanism of selective inhibition of the inducible isoform of prostaglandin G/H synthase. Proc. Natl. Acad. Sci. U.S.A. 91, 11202–11206.

Cuzzocrea, S., Sautebin, L., De Sarro, G., Costantino, G., Rombola, L., Mazzon, E., Ialenti, A., De Sarro, A., Ciliberto, G., Di Rosa, M., Caputi, A.P., Thiemermann, C., 1999. Role of IL-6 in the pleurisy and lung injury caused by carrageenan. J. Immunol. 163, 5094–5104.

Cuzzocrea, S., Riley, D.P., Caputi, A.P., Salvemini, D., 2001. Antioxidant therapy: a new pharmacological approach in shock, inflammation, and ischemia/reperfusion injury. Pharmacol. Rev. 53, 135–159.

Feuerstain, G., Hallenbeck, J.M., 1987. Prostaglandins, leukotrienes, and platelet-activating factor in shock. Ann. Rev. Pharmacol. Toxicol. 27, 301–313.

Futaki, N., Yoshikawa, K., Hamasaka, Y., Arai, I., Higuchi, S., Iizuka, H., Otoma, S., 1993. NS-398, a novel non-steroidal anti-inflammatory drug with potent analgesic and antipyretic effects, which causes minimal stomach lesions. Gen. Pharmacol. 24, 105–110.

Gans, K.R., Galbraith, W., Romans, R.J., Haber, S.B., Kerr, J., Schmidt, W.K., Smith, C., Hewes, W.E., Ackerman, N.R., 1990. Anti-inflammatory and safety profile of DuP 697, a novel orally effective prostaglandin synthesis inhibitor. J. Pharmacol. Exp. Ther. 254, 180–187.

Guarnieri, F., Still, W.C., 1994. A rapidly convergent simulation method: mixed Monte Carlo/Stochastic dynamics. J. Comput. Chem. 15, 1302–1310.

Kosaka, T., Miyata, A., Ihara, H., Hara, S.S., Sugimoto, T., Takeda, O., Takahashi, E., Tanabe, T., 1994. Characterization of the human gene (PTGS2) encoding prostaglandin-endoperoxide synthase 2. Eur. J. Biochem. 221, 889–897.

Kurumbail, R.G., Stevens, A.M., Gierse, J.K., McDonald, J.J., Stegeman, R.A., Pak, J.Y., Gildehaus, D., Miyashiro, J.M., Penning, T.D., Seibert, K., Isakson, P.C., Stallings, W.C., 1996. Structural basis for selective inhibition of cyclooxygenase-2 by anti-inflammatory agents. Nature 384, 644–648.

Laight, D.W., Lad, N., Woodward, B., Waterfall, J.F., 1994. Assessment of myeloperoxidase activity in renal tissue after ischemia/reperfusion. Eur. J. Pharmacol. 292, 81–88.

McDonald, D.Q., Still, W.C., 1992. AMBER* torsional parameters for the peptide backbone. Tetrahedron Lett. 33, 7743–7746.

Mitchell, J.A., Larkin, S., Williams, T.J., 1995. Cyclooxygenase-2: regulation and relevance in inflammation. Biochem. Pharmacol. 50, 1535–1542.

Mohamadi, F., Richards, N.G.J., Guida, W.C., Liskamp, R., Lipton, M., Caufield, C., Chang, G., Hendrick-son, T., Still, W.C., 1990. Macro model—an integrated software system for modeling organic and bioorganic molecules using molecular mechanics. J. Comput. Chem. 11, 440–467.

Ohkawa, H., Ohishi, H., Yagi, K., 1979. Assay for lipid peroxides in animal tissues by thiobarbituric acid reaction. Anal. Biochem. 95, 351–358.

Ottanà, R., Monforte, F., Alcaro, S., De Luca, G., Maccari, R., Ortuso, F., Vigorita, M.G., 2001. First Magna Græcia Medicinal Chemistry Workshop on New Perspectives in Drug Research June 10–13, 2001, Copanello (CZ, Italy); Abstr. PC40.

Palomer, A., Perez, J.J., Naveae, S., Llorens, O., Pascual, J., Garcia, L., Mauleon, D., 2000. Modeling cyclooxygenase inhibition. Implication of active site hydration on the selectivity of Ketoprofen analogues. J. Med. Chem. 43, 2280–2284.

Patrono, C., Ciabattoni, G., Pugliese, F., Pinca, E., Castrucci, G., De Salvo, A., Cattani, P., 1980. Radioimmunoassay measurement of stable metabolites of platelet arachidonic acid: a convenient method for the in vitro and ex vivo evaluation of cyclo-oxygenase inhibitors. Agents Actions Suppl. 7, 256–259.

Picot, D., Loll, P.J., Garavito, R.M., 1994. The X-ray crystal structure of the membrane protein prostaglandin H_2 synthase-1. Nature 367, 243–249.

Previtera, T., Vigorita, M.G., Basile, M., Fenech, G., Trovato, A., Occhiuto, F., Monforte, M.T., Barbera, R., 1990. 3,3′-Di[1,3-thiazolidine-4-one]

system. V. Synthesis and pharmacological properties of 3,3′(1,2-ethanediyl)bis[2-heteroaryl-1,3-thiazolidine-4-one] derivatives. Eur. J. Med. Chem. 2, 569–579.

Raz, A., Wyche, A., Needleman, P., 1989. Temporal and pharmacological division of fibroblast cyclooxygenase expression into transcriptional and translational phases. Proc. Natl. Acad. Sci. U.S.A. 86, 1657–1661.

Renz, H., Gong, J.H., Schmidt, A., Nain, M., Gemsa, D., 1988. Release of tumor necrosis factor-alpha from macrophages. Enhancement and suppression are dose-dependently regulated by prostaglandin E_2 and cyclic nucleotides. J. Immunol. 141, 2388–2393.

Ristimaki, A., Garfinkel, S., Wessendorf, J., Maciag, T., Hla, T., 1994. Induction of cyclooxygenase-2 by interleukin-1 alpha. Evidence for post-transcriptional regulation. J. Biol. Chem. 269, 11769–11775.

Sautebin, L., Ialenti, A., Ianaro, A., Di Rosa, M., 1995. Modulation by nitric oxide of prostaglandin biosynthesis in the rat. Br. J. Pharmacol. 114, 323.

Simon, L.S., Lanza, F.L., Lipsky, P.E., Hubbard, R.C., Talwalker, S., Schwarz, B.D., Isakson, P.C., Geis, G.S., 1998. Preliminary study of the safety and efficacy of SC-58635, a novel cyclooxygenase 2 inhibitor: efficacy and safety in two placebo-controlled trials in osteoarthritis and rheumatoid arthritis, and studies of gastrointestinal and platelet effects. Arthritis Rheum. 41, 1591–1602.

Theisen-Popp, P., Pape, H., Muller-Paddinghaus, R., 1992. Interleukin-6 (IL-6) in adjuvant arthritis of rats and its pharmacological modulation. Int. J. Immunopharmacol. 14, 565–571.

Tomlinson, A., Appleton, I., Mooregilroy, A.R., Willis, D., Mitchell, J.A., Willoughby, A., 1994. Cyclo-oxygenase and nitric oxide synthase isoforms in rat carrageenin-induced pleurisy. Br. J. Pharmacol. 113, 693–698.

Vane, J.R., 1987. Anti-inflammatory drugs and the many mediators of inflammation. Int. J. Tissue React. 9, 1–14.

Vane, J.R., Mitchell, J.A., Appleton, I., Tomlinson, A., Bishop-Bailey, D., Croxtall, J., Willoughby, D.A., 1994. Inducible isoforms of cyclooxygenase and nitric-oxide synthase in inflammation. Proc. Natl. Acad. Sci. U.S.A. 91, 2046–2050.

Vigorita, M.G., Previtera, T., Basile, M., Fenech, G., Costa De Pasquale, R., Occhiuto, F., Circosta, C., 1988. 3,3′-Di[1,3-thiazolidine-4-one] system. IV. Synthesis and pharmacological properties of 3,3′-(1,2-ethanediyl)-bis[2-aryl-1,3-thiazolidine-4-one 1,1′dioxide] derivatives. Il Farmaco. 4, 373–379.

Vigorita, M.G., Previtera, T., Ottanà, R., Grillone, I., Monforte, F., Monforte, M.T., Trovato, A., Rossitto, A., 1997. 3,3′-Bi(1,3-thiazolidin-4-one) system. IX. Synthesis of racemic and meso. 3,3′-(1,2-ethanediyl)bis[2-aryl-4-thiazolidinone] derivatives and corresponding 1,1′-disulfones. Evaluation of anti-inflammatory and related activities. Il Farmaco. 52, 43–48.

Vigorita, M.G., Ottanà, R., Monforte, F., Maccari, R., Trovato, A., Monforte, M.T., Taviano, M.F., 2001. Synthesis and anti-inflammatory, analgesic activity of 3,3′-(1,2-ethanediyl)bis[2-aryl-4-thiazolidinone] chiral compounds. Part 10. Bioorg. Med. Chem. Lett. 11, 2791–2794.

Warner, T.D., Giuliano, F., Vojnovic, I., Bukasa, A., Mitchell, J.A., Vane, J.R., 1999. Nonsteroid drug selectivities for cyclo-oxygenase-1 rather than cyclo-oxygenase-2 are associated with human gastrointestinal toxicity: a full in vitro analysis. Proc. Natl. Acad. Sci. U.S.A. 96, 7563–7568.

Yokohama, C., Tanabe, T., 1989. Cloning of human gene encoding prostaglandin endoperoxide synthase and primary structure of the enzyme. Biochem. Biophys. Res. Commun. 165, 888–894.